Design and optimisation of low heat load liquid helium cryostat to house cryogenic current comparator in antiproton decelerator at CERN

Design and optimisation of low heat load liquid helium cryostat to house cryogenic current comparator in antiproton decelerator at CERN

A. Lees, T. Koettig, M. Fernandes, J. Tan

CERN, Accelerator Technology Department, CH-1211 Geneva 23, Switzerland

Andrew.Lees@cern.ch

Abstract. The Cryogenic Current Comparator (CCC) is installed in the low-energy Antiproton Decelerator (AD) at CERN to make an absolute measurement of the beam intensity. Operating below 4.2 K, it is based on a superconducting quantum interference device (SQUID) and employs a superconducting niobium shield to supress magnetic field components not linked to the beam current. The AD contains no permanent cryogenic infrastructure so the local continuous liquefaction of helium using a pulse-tube is required; limiting the available cooling power to 0.69 W at 4.2K. Due to the sensitivity of the SQUID to variations in magnetic fields, the CCC is highly sensitive to mechanical vibration which is limited to a minimum by the support systems of the cryostat. This article presents the cooling system of the cryostat and discusses the design challenges overcome to minimise the transmission of vibration to the CCC while operating within the cryogenic limits imposed by the cooling system.

1. Introduction

The CCC cryostat is installed in the antiproton decelerator (AD) at CERN and houses the toroidal shaped cryogenic current comparator (CCC). The CCC uses a superconducting quantum interference device (SQUID) to calculate the AD beam intensity by measuring the distribution of its magnetic field [1] [2]. The SQUID, which is highly sensitive to mechanical vibrations [3], and the niobium shielding structure of the CCC are immersed in liquid helium (LHe) supplied by a pulse-tube reliquefier. The main design challenge was to optimize the thermal and mechanical performance of the cryostat to retain a stable amount of LHe while minimizing the transmission of vibrations to the CCC.

Design, manufacture, installation and commissioning of the project was achieved in line with operational schedule of the AD during a twelve month period finishing in June 2015. Since this time the CCC has proven to be a useful beam diagnostic tool [1], however limited thermal performance has reduced its availability. Several likely areas contributing to the reduced thermal performance have been identified initiating an upgrade to the multi-layer insulation of the cryostat, planned during the first half of 2016.

2. Cryostat design

As shown in figures 1 and 2 the cryostat is comprised of three main assemblies; helium vessel (HV), thermal radiation shield (TS) and vacuum vessel (VV), which are toroidal in shape and aligned horizontally. The HV and VV are made from 316LN stainless steel (CERN grade) [4] due to its low magnetic permeability at cryogenic temperatures [5] [6]. The TS is copper reinforced with stainless steel ribs to reduce vibration, its cooling circuit is also copper and braised into position. The concentric beam tubes of the HV, TS and VV pass horizontally 57 mm below the axis of the cryostat outer diameter, the standard AD beam tube diameter of 150 mm is reduced to 103 mm to allow the beam tubes to fit through the 185 mm inner diameter of the CCC. Protected from thermal stress by flexible bellows electrically insulating ceramic isolators [7] are integrated into the HV and VV beam tubes to prevent the mirror currents induced by the AD beam shielding the magnetic field signal from the CCC. The TS includes a 4mm gap to provide electrical insulation between the beam tube and front door, which is fixed mechanically with a clamp made from Ultem1000®. 1 mm thick perforated tubes made from G10 were used to internally support multi-layer insulation (MLI) inside the HV and TS beam tubes where clearances of 7 mm and 10 mm respectively mean assembly tolerances are small. To match the thermal

expansion of the CCC's niobium shielding and avoid thermal stress it is clamped into a grade 2 titanium collar and connected to the HV with four flexible stainless steel plates. The SQUID cables are routed to their data acquisition equipment through a dedicated feedthrough (SF) between the VV and HV, shown in figures 1 and 5. Extending from the top of the cryostat is the heater turret (HT) housing an electric heater (EH) and acting as a terminal for the cooling circuit and safety valve line (SV line) from the HV.

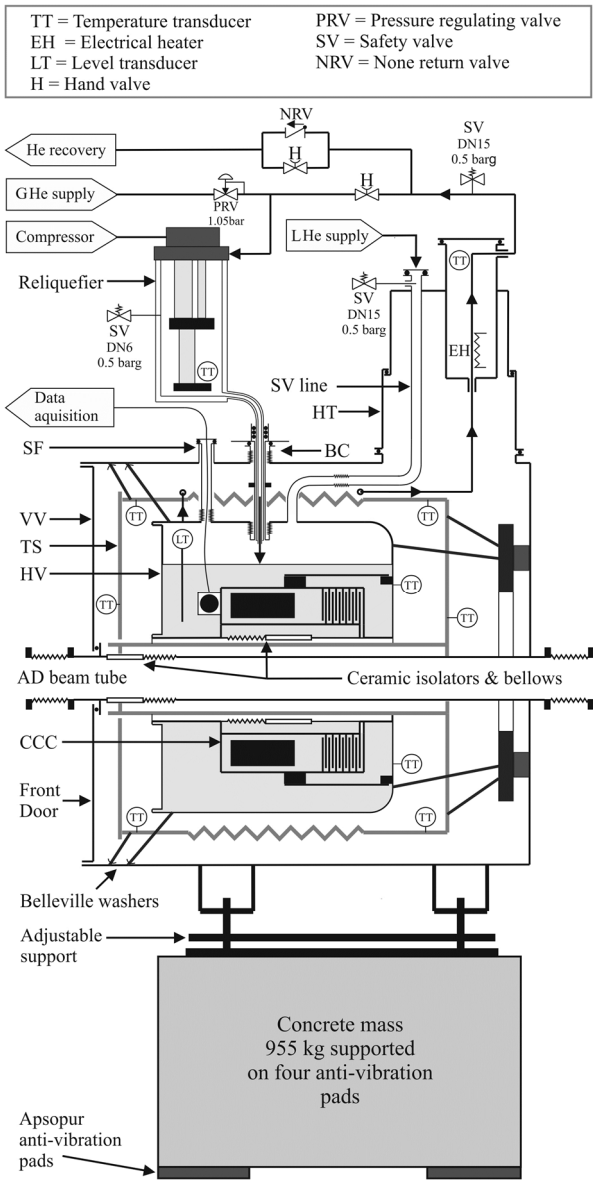

Figure 1. CCC Cryostat schematic

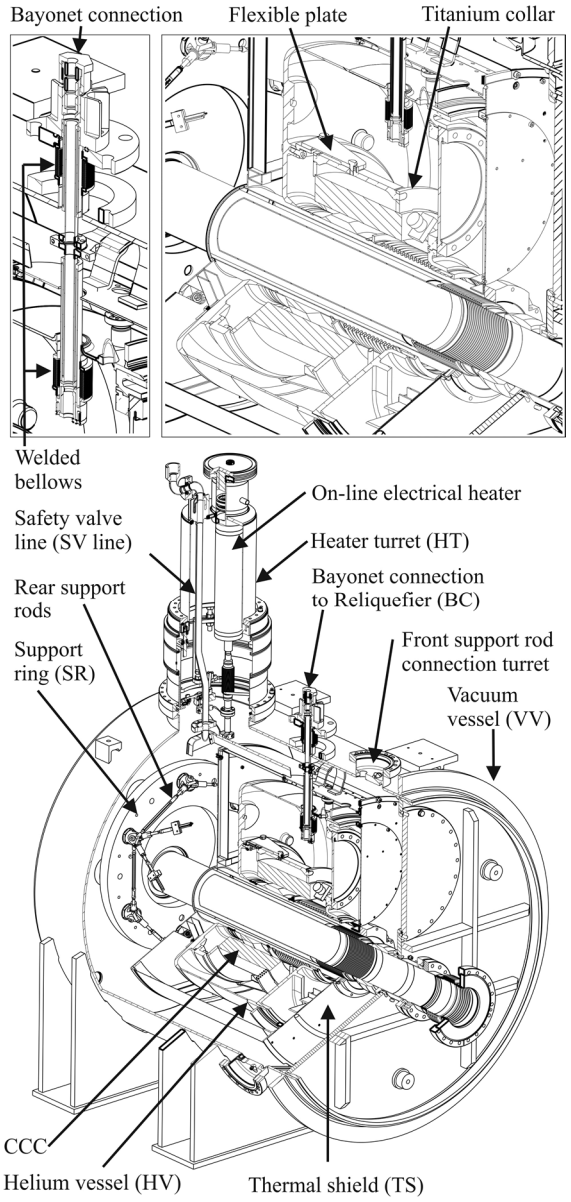

Figure 2. CCC Cryostat Detailed Drawing

2.1. Thermal design

To reduce the vibration transmitted to the CCC a Cryomech® PT415 helium reliquefier was used in place of an integrated pulse tube and connected to the cryostat using a bayonet connection (BC) designed to mechanically isolate the two systems as shown in figures 1 and 2. The standard PT415 pulse tube generates a cooling power of 1.5 W at 4.2 K [8]; when used as part of the reliquefier it can liquefy up to 15 liters of helium per day from room temperature or re-liquefy up to 27 liters of cold helium per day from a cryostat [9], equating to cooling powers of 0.45 W and 0.81 W respectively at 4.2 K.

The cooling circuit is shown in figure 1; to reduce thermal radiation on the HV cold evaporated helium passes through the TS cooling circuit, however as the helium must be heated to room temperature using the on-line electrical heater the efficiency of the reliquefier is reduced. To improve efficiency a

proportion of the cold evaporated helium can return directly to the reliquefier through the BC as in the case of a cryostat, this flow is limited by the pressure drop caused by the counter flow of LHe. Warming of the HV increases helium flow and cooling of the TS reducing heat load on the HV, this negative feedback loop causes the system to tend towards a stable temperature with the reliquefier producing an effective cooling power somewhere between its two operational modes.

Table 1 shows the calculated heat loads on the HV and TS; in both cases thermal conduction through the support rods is the highest heat load, although radiation to the TS is also significant. The HV support rods, BC, SF and SV line are thermalized to the TS using copper braid with a cross-section of 50 mm² and a maximum length of 80 mm, this significantly reduces heat load on the HV but increases the heat load on the TS. The calculated heat load on the HV of 0.57 W creates an evaporated gas flow of 0.028 g/s, the enthalpy of helium between 5 K and 75 K gives 10.2 W of power available to cool the TS. The cooling pipe of the TS has an internal diameter of 10 mm giving a flow velocity of 0.49 m/s and a logarithmically averaged heat exchange coefficient of 20.64 W/m²K. The length of TS cooling circuit is 6.8 m which is more than enough to take advantage of the cooling power available and ensure that with 9.17 W heat load on the TS the temperature should be stable below 75 K.

During operation the distribution of gas flow between the TS cooling circuit and the BC can be biased by a hand valve on the TS return line to the reliquefier. The system operates slightly above atmospheric pressure with a maximum allowable pressure of 0.5 barg, limited by the ceramic isolator in the HV beam tube [7]. Any overpressure in the circuit is released and returned to the helium recovery line through the pressure relief valve.

Table 1. Heat load on HV and TS

	TS (W)	HV (W)
Thermal Radiation	2.84[a]	0.12[b]
Support Rods	4.61[cd]	0.26[d]
Bayonet Connection	0.49[ce]	0.05[e]
SV line	0.56[ce]	0.02[e]
SQUID Feedthrough	0.53[ce]	0.06[e]
Instrumentation	0.06[f]	0.04[f]
Heater Line	0.09[e]	0.01[e]
Total	9.17	0.57

[a] Assumed heat flux of 1.2 W/m² on outer diameter and end faces (25 layers of MLI) and 3.1 W/m² on beam tube (10 layers of MLI).

[b] Assumed heat flux of 0.1 W/m² (10 layers of MLI).

[c] All or part of heat load brought to TS through thermal intercept (copper braid).

[d] Integral thermal conductivity calculated from [10].

[e] Integral thermal conductivity calculated from [11].

[f] Including SQUID cable and manganin cryogenic instrumentation cables.

2.2. Mechanical design

The main source of vibration is the reliquefier itself; the pulse tube and compressor creating harmonic oscillations at 1 to 2 Hz and 50 Hz respectively. The AD complex contains vibrating machines close to the cryostat; previous studies have measured ground born harmonic vibrations of 50 Hz with amplitude up to 30 nm and single impact events creating vibrations up to 80 nm [12]. It is also possible that low amplitude vibrations could be transmitted through the AD beam tube. Due to the mechanical and cryogenic connections between the HV, TS and VV it is not possible to isolate them from each other. Firstly it is not possible to isolate frequencies as low as 1 to 2 Hz, secondly making all connections flexible would allow the HV to move due to changes of pressure in the helium circuit. For this reason the support system is designed to isolate external vibration to the VV and then avoid the resonance of the HV and TS by increasing the stiffness of their supports.

The mass of the HV is 145 kg (including 55 kg for the CCC) and the mass of the TS is 55 kg, they are supported using independent sets of twelve support rods, see figure 3. G10, Kevlar 49®, titanium and stainless steel were considered as possible materials for the support rods, figure 4 shows a comparison of the ratio of Young's modulus to thermal conductivity for each material. G10 is well suited to this application however its low stiffness requires a minimum cross-sectional area of 80 mm² for each support rod, which was difficult to integrate into the design. Kevlar 49® is also ideally suited, however load-deflection testing on 3 and 4 mm diameter cord found a stiffness much lower than the theoretical value due to void fraction, fiber angle and the uneven distribution of loading across the fibers. With no time available for further development it was decided to use grade 5 titanium (6%Al-4%V), which has

a better stiffness to thermal conductivity ratio that stainless steel. A cross sectional area of 20 mm² was used for each support rod and their geometry optimized to increase the first vibrational modes of the HV and TS to 64.7 Hz and 68.1 Hz respectively, while minimizing heat loads from conduction.

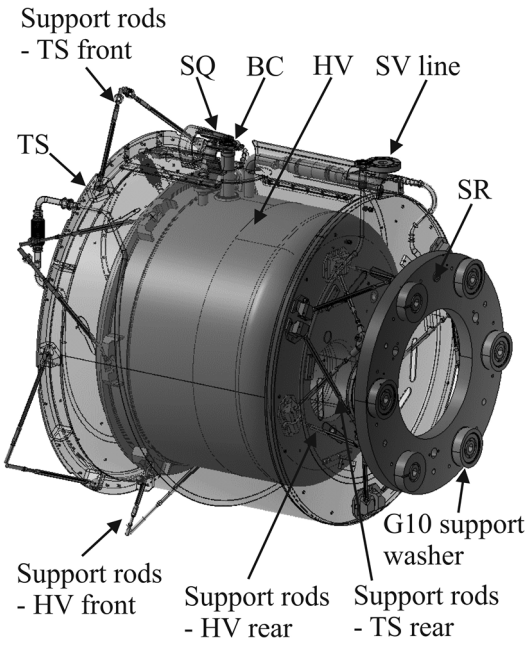

Figure 3. HV and TS with titanium support rods and rear support ring

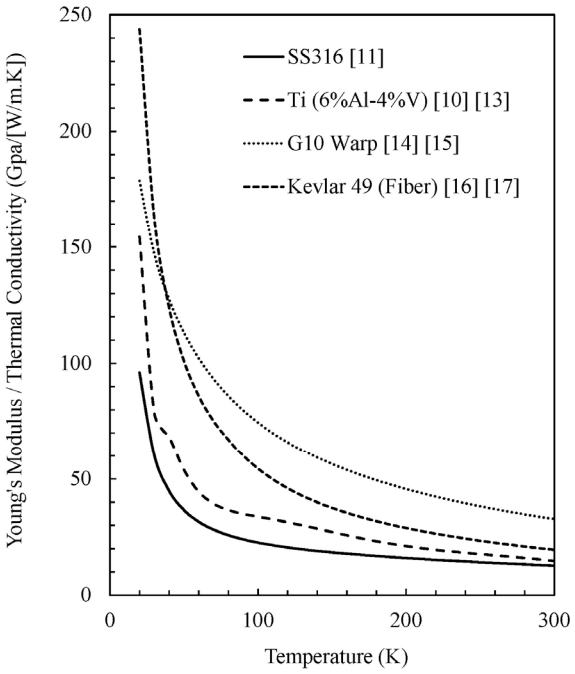

Figure 4. Support materials: Comparison of Young's modulus to thermal conductivity

To allow for thermal shrinkage, Belleville washers were fitted to the warm end of the rods near the front door of the cryostat. To avoid reducing the stiffness of the support rods detailed mechanical analysis was undertaken to ensure that the Belleville washers were fully flattened during cool down and that the thermal stresses created in the support rods and cryostat were acceptable. The use of titanium helped in this respect as its high yield strength gave a comfortable margin to account for artificially high pre-loading of the support rods due to assembly errors.

To isolate the 850 kg cryostat assembly from ground borne vibration it is mounted on a 955 kg concrete mass and four Apsopur® anti-vibration mats [18], a configuration which is calculated to isolate 92 % of vibrations at 50 Hz. The first mode of the cryostat assembly is reduced to 4.7 Hz and its main vertical bounce mode to 12.7 Hz, strategically placed between the forcing frequencies of the reliquefier and well below the vibrations from AD infrastructure and the resonant frequencies of the HV and TS.

As shown in figure 5, to decouple its vibration from the cryostat the reliquefier is supported on a stiff aluminum bridge. During operation the upper flange of the BC is connected directly to the aluminum bridge, leaving its welded bellows as the only transfer paths between the reliquefier and the cryostat, also shown in figure 2. The reliquefier is mounted into a vertically sliding support system to allow easy installation of its drainage leg into the BC.

The cryostat is isolated from the vibrations of the AD beam tube with flexible bellows on both sides.

3. Manufacture and assembly

The HV, TS, VV and HT were manufactured by CERN's central workshop who have experience of 316LN stainless steel and the braising techniques required for the TS and piping connections. The titanium support rods and their connections were outsourced to Thompson Precision based in the UK.

Assembly took place in parallel to the final phase of manufacture and was also managed by CERN's central workshop, enabling the project to meet the AD operational schedule. The procedure began with the installation of the CCC in the HV, followed by the mounting of its instrumentation and MLI. With the beam pipes aligned vertically the TS was mounted over the HV, its instrumentation and MLI installed before the rear support rods and support ring were mounted above. Using the support ring the

HV and TS were then pulled vertically into the VV and the front support rods connected. Once the piping between components was connected the VV beam pipe was installed and the cryostat oriented horizontally. Finally the front door was welded shut and the HT mounted in position, the whole process was completed in less than four weeks including leak tests and the final pressure test.

Several aspects of the assembly proved challenging; the 24 support rods and 3 piping connections required holes to pass though the MLI of the TS, it was also difficult to incorporate the thermalizing copper braids into the MLI in a satisfactory manner. To verify the pre-loading of the support rods and monitor loading during cool down a strain gauge was fitted to each rods. During assembly the routing and material of the strain gauge cables was incorrectly specified, introducing extra heat load on the TS.

4. Testing

During commissioning the cryostat was directly filled with LHe, some thermo-acoustic oscillations were observed in the helium circuit. Throughout cooldown the loads on the support rods followed closely those predicted by analysis, verifying that the Belleville washers were fully flattened. Once full the supply of LHe to the HV was removed and the LHe level monitored for two hours, at this time the reliquefier was activated. Figure 6 shows the reducing level of LHe indicating a heat load of 1.04 W on the HV and that the reliquefier produced a cooling power of 0.69 W at 4.2 K. While the TS temperature was below 100 K the LHe level was relatively stable, however the TS temperature continued to rise to 128 K, 55 K higher than expected. By integrating a membrane pump and flow meter into the cooling circuit it was possible to estimate the heat load on the TS as 16 W, 6.83 W higher than anticipated.

5. Conclusions

High heat load on the TS allows only five days of operation before the LHe level in the HV is too low for the CCC to function. Based on this performance the cryostat was still integrated into the AD complex and filled monthly to enable the proof of concept of the CCC detector. The mechanical behavior of the cryostat during cooldown and operation has been as intended, CCC measurements have shown mechanical noise to be hidden below the current level of electromagnetic noise recorded and no resonance has been noted.

Investigations have indicated that high heat load on the TS is most likely to be caused by the routing and material of the strain gauge cables, thermal radiation passing through the MLI where it is cut to allow the passage of support rods and piping, the lack of MLI on the support rods themselves and finally the high emissivity of the G10 used to support MLI on the HV and TS beam tubes.

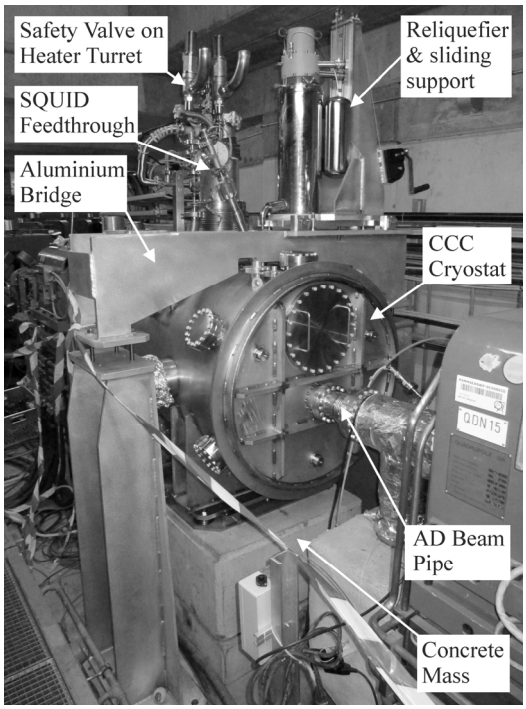

Figure 5. CCC Cryostat installed in AD

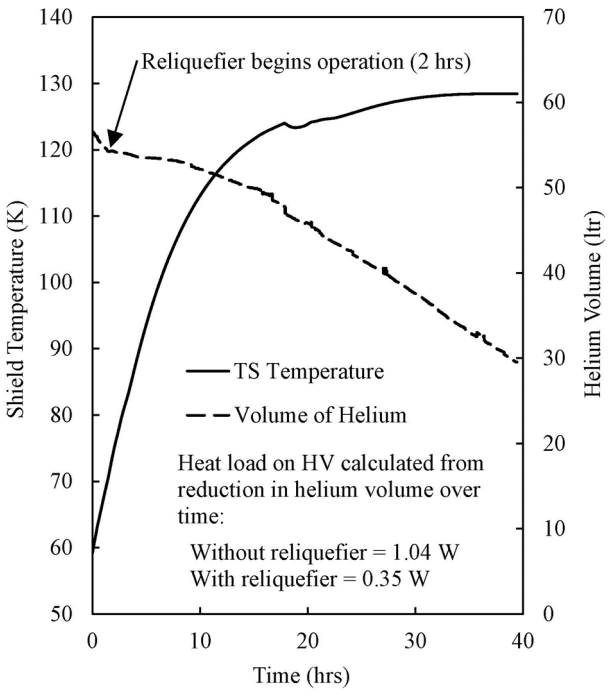

Figure 6. Cold test: LHe level and TS temperature

To correct these issues the cryostat will be removed from the AD complex during the 2016 technical stop. The strain gauges and their cable are no longer required so can be removed and the MLI will be upgraded, addressing the issues listed above to reduce radiative heat load on the TS and HV. It is also thought that the addition of a membrane pump to stabilize the flow rate in the TS cooling circuit may improve overall performance.

6. Acknowledgments

The authors would like to thank their colleagues in CERN's engineering department, central workshop, cryogenic laboratory, vacuum department and AD complex who assisted in the design, manufacture, assembly and installation of the CCC cryostat. We would also like to thank GSI and Jena for the loan of the CCC detector and their ongoing collaboration.

References

[1] Fernandes M, Tan J, Welsch C P, Geithner R, Neubert R, Schwickert M, Stöhlker T, "A cryogenic current comparator for the low energy antiproton facilities at CERN", *International Beam Instrumentation Conference*, Melbourne, Australia, 13-17 September 2015, pp.MOPB043

[2] Geithner R, Neubert R, Vodel W, Schwickert M, Reeg H, von Hahn R, Seidel P, "A Non-Destructive Beam Monitoring System Based on an LTS-SQUID", Applied Superconductivity, IEEE Transactions, Volume: 21, Issue: 3, June 2011, pp. 444 – 447.

[3] A. Peters, H. Reeg, C.H. Schroeder, W. Vodel, H. Koch, R. Neubert, H. Muehlig, "Review of the Experimental Results with a Cryogenic Current Comparator", Proceedings of the 5th EPAC , June 1996, Sitges, Spain, pp. 1627-1629

[4] CERN Specification, "Stainless steel sheets/plates for ultra-high cacuum applications, 1.4429 AISI 316LN", CERN Engineering Department, Geneva, switzerland, EDMS No. 790774.

[5] 1974, *Materials for cryogenic service: Engineering properties of austenitic stainless steel*, Nickel Development Institute courtesy of Inco ltd, Pub no. 4368, pp. 6.

[6] Couturier K, Sgobba S, "Phase stability of high manganese austenitic steels for cryogenic applications", *Materials Week 2000 Conference*, Munich, Germany, 25-28 September 2000.

[7] Drawing of ceramic isolator FA30393CA, Solid sealing technolocg Inc. http://www.solidsealing.com

[8] PT415 Pulse tube cryorefrigerator specification sheet, Cryomech Inc. http://www.cryomech.com.

[9] PT415 Helium Reliquefier specification sheet, Cryomech Inc. http://www.cryomech.com.

[10] Ziegler W T, Mullins J C, Hwa S C P, "Specific heat and thermal conductivity of four commercial titanium alloys from 20 to 300 K, *Advances in cryogenic engineering vol 8*, University of California, Los Angeles, US, August 14-16, 1963, pp. 268-277.

[11] Mann D 1977, *LNG materials and fluids*, National bureau of standards and tecnology (NIST), Cryogenic division, US, chart 1016.

[12] Sylte M, "Ground motion measurements for the AEGIS experiment", CERN Engineering Department, Geneva, Switzerland, EDMS No. 1028826, 05 October 2009, unpublishd.

[13] Ekin J W 2006, *Experimental Techniques for Low-Temperature Measurements*, Oxford University Press Inc., New York, United States, pp. 258.

[14] Veres, H.M., *Thermal Properties Database for Materials at Cryogenic Temperatures*. Vol 1.

[15] Kasen M B, MacDonald G R, Beekman D H, Schramm R E, " Mechanical, electrical and thermal characterization of G-10CR and G-11cr glass-cloth/epoxy laminates between room temperature and 4 k", *Advances in cryogenic engineering vol 26*, Madison, Wisconsin, 1980, pp. 235-244.

[16] Ventura G, Martelli V, "Thermal conductivity of kevlar 49 between 7 and 290 K", *Cryogenics 49*, 2009, pp. 735-737.

[17] Schutz J B, "Properties of composite materials for cryogenic applications", *Cryogenics 38*, January 1998, pp. 3-12.

[18] Apsopur antivibration mat data sheet, Angst+Pfister Inc. http://www.angst-pfister.com